I S A V

Journal of Theoretical and Applied Vibration and Acoustics

journal homepage: http://tava.isav.ir

Experimental identification of parameters for joint affected region in an under-platform damper

Shayan Eini[a], **Mehrdad Motavasselolhagh**[b], **Majid Rajabi**[c*]

[a] *M.Sc. Student, School of Mechanical Engineering, Iran University of Science and Technology, Tehran, IRAN*

[b] *Ph.D. Student, School of Mechanical Engineering, Iran University of Science and Technology, Tehran, IRAN*

[c] *Associate Professor, School of Mechanical Engineering, Iran University of Science and Technology, Tehran, IRAN*

ARTICLE INFO

Article history:
Received 18 October 2021

Received in revised form
7 November 2021

Accepted 11 March 2022

Available online 25 June 2022

Keywords:
System identification,

Joint affected region,

Model updating,

Under-platform damper,

Friction and contact.

ABSTRACT

The primary objective of this research is to identify the physical and geometrical properties of the joint-affected region in under-platform dampers and minimize errors caused by the selection of the contact surface type by updating the connection properties. Additionally, an optimized model is proposed for selecting the type of finite element to reduce execution time using system simulation in finite element software. The experimental test has been done on the three-dimensional model of two blades with the under-platform damper in a free-free manner, and the behavior of the joint-affected region has been optimized according to the results extracted from the experimental test. Three types of affected regions, rectangular, and ellipsoidal, and two pieces shapes, are considered in five different dimensions to obtain the best model and dimensions of the affected surface.

The ellipsoidal model yields simulation results that are closer to the experimental test results with lower error. Moreover, reducing the dimensions of the affected surface to the center of the effect provides more accurate results. These findings have significant implications for improving the performance of under-platform dampers and reducing vibrations in mechanical structures.

© 2022 Iranian Society of Acoustics and Vibration, All rights reserved.

1. Introduction

Aircraft engines operate in various conditions during flight, making it impossible to avoid all important resonances in aviation engine-bladed disks [1]. By lowering the risk of high cycle fatigue brought on by high resonant stresses, minimizing vibration at these resonant frequencies is the primary way to guarantee the longevity and dependability of aviation engines. Dry friction

* Corresponding author:
E-mail address: majid_rajabi@iust.ac.ir (M. Rajabi)

http://dx.doi.org/10.22064/tava.2023.563667.1214

damping is a popular technique for reducing vibration in a bladed disk because it offers excellent damping at a cheap cost through rubbing action on contact surfaces [2].

Dry friction damping, which results from the rubbing motion between contact surfaces, can effectively convert vibrational energy into heat energy and reduce fatigue stress levels [3]. The location of the dry friction damper is also critical. There are various locations of dry friction dampings in bladed disks namely root joints, blade tip, and shroud which are shown in Figures 1(a) to 1(c), respectively. Among these, the under-platform damper is one of the most effective ways to increase vibrational energy dissipation by enhancing damping in the system.

Typically located on the underside of the platform between adjacent blades [red circles in Figure 1(c)], under-platform dampers are compactly held in place under the action of centrifugal force. The impact of airflow on the blades results in circumferential vibrations of the blade roots, which in turn create relative motion between the under-platform damper and the platform. The damper, pressed onto the platform by centrifugal force, experiences friction and deformation at the contact surface due to the relative motion. This conversion of mechanical energy into heat energy reduces the amplitude of the blade to a lower level, thereby reducing vibrational stress in the blade structure and improving blade fatigue life.

The interaction friction between the platform and damper is strongly nonlinear, resulting in complex dynamic behavior due to stick-slide and separation conditions. Numerous researchers have therefore focused on describing this complex dynamic problem while considering tribology.

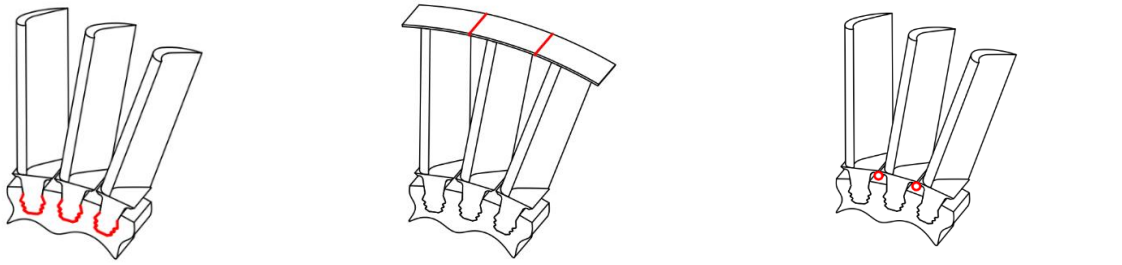

(a) Root joints (b) Blade tips (c) Under-platform damper

Fig. (1) Different locations of dry friction damping [3].

The most popular type of friction damper used in turbine discs are under-platform dampers. Under-platform dampers are metal components that are typically positioned in the groove beneath the neighboring two-blade platforms. During operation, centrifugal stresses bring the under-platform dampers into contact with the platforms. The relative movement between the platforms and the damper, which occurs when the vanes vibrate, causes friction on the contact surfaces, which results in considerable energy loss and a decrease in the resonance amplitude. The dynamic response of the finned disk outfitted with under-platform dampers is very nonlinear as a result of the frictional nature of this issue, and the number of vibrations and resonance frequencies relies on the amplitude [4].

In many studies, the assembly of the blade-disk damper is simplified to a basic contact structure. For instance, the blade and its platform are often reduced to a flat plate and a boss on the blade root in the three-dimensional model, with the resulting projection on the x-y plane. Figures 2(a)

and 2(b) illustrate the two common types of under-platform dampers used in aero-engines, namely the plane shape and the wedged shape, respectively [3].

(a) Plan shape (b) Wedged shape

Fig. (2) The structure of under-platform damper [3].

By simulating the turbine blade as a single degree of freedom with Coulomb friction, Griffin was able to effectively investigate turbine blade resonance analysis with a ground-blade coupled damper [5]. An approach to designing friction dampers for high-speed turbomachines was put out by Cameron *et al* [6]. Cigeroglu enhanced his friction damper model as a part of his ongoing research. By presenting a generic two-dimensional model and employing the criteria Cigeroglu was able to pinpoint the limits of adhesion, sliding, and separation in a rod and a turbine blade [7]. Sanliturk et al stated that the main feature of the microslip phenomenon is that with increasing displacement the slope of the force-displacement curve decreases. It defines their appearance by defining a model [8]. Some more comprehensive models considering the vertical force were developed by Yang *et al*. They developed a criterion of passing through the adhesion-sliding-detachment state while it is subjected to a vertical force [9]. Later, Cigeroglu utilized various criteria introduced for the exact solution of a rod. The proposed model is a continuum model of friction where the effect of inertia is considered. This model, considering the inertia of the rod, for two vertical forces, convex and concave under axial loading, developed the continuum model proposed by Menq [10]. In their new work, Sunlitrak *et al.* [11] used experimentally measured contact characteristics to model friction contact. To simplify the model, they omitted the dampers flexibility and inertia effects. Instead, their focus was on the relative displacemens at contact points and a static analysis of the forces, by applying the harmonic balance method to linearize these forces. They calculated the equivalent dumping and stiffness. Ozguven and Cigeroglu diagram hysteresis was approximated by two slopes. In this method, the return path of the hysteresis diagram is approximated by two lines, each one independently. Their goal was to offer an accurate yet simple model that can be easily used in the design of friction dampers [12]. Allara introduced a model for contact friction for non-spherical geometries to calculate hysteresis curves of tangential contact force and relative tangential displacements [13].

Several methods have been developed during the last few decades to simulate the dynamics of structures coupled to frictional contacts. The most basic models include mass, a linear spring, and parallel and non-linear series components including springs, dampers, and Columbus friction sliders [4].

Following the results of the current research, the researchers attempted to accurately model the friction by first presenting an appropriate friction model. Then, using a variety of proposed friction models, they attempted to ascertain the dynamic behavior of the turbine blades in actual models or in models that studied large and complex finite elements. The offered models cannot be employed

in the modeling of the dynamic movement of turbine blades with a hut roof damper, either because they are not complete or because they include specific parameters such as spherical geometry. These models are ideal for determining friction forces, despite the comprehensive nature of other models that come with various complexities.

This study uses the findings of vibration testing to identify and explore the elastic behavior and characteristics of connections in the turbine blade. For structural connections, a connection-affected region is designated with this in mind. This region comprises a narrow layer with unidentified isotropic characteristics, including the elastic modulus E and Poisson's ratio v.

In this paper, experimental identification of parameters of the area under the influence of under-platform damper connection is considered. First, the joint affected region connection modeling technique and the case study are fully explained. Then, the design process of finite element models using the joint affected region technique is explained. Experimental modal testing is used to study and identify connection properties by extracting the Frequency Response Function (FRF) of the natural frequencies of the system. Finally, a cost function is defined as the error between measured and numerically modeled natural frequencies. By optimizing this cost function, the parameters of the system are identified and the best connection type is found.

2. Joint Affected Region (JAR)

The interface layer model is a fresh method that was recently suggested to mimic the dynamic behavior of interface surfaces [14]. The idea of the zone under the impact of connection serves as the foundation for this model, which is schematically depicted in Figure 3. It is expected that a portion of the substructures will be affected by the effect of lowering the stiffness of the screw connection. As a result, the region affected by the connection is thought to be a comparable region around the interface region. This area's thickness is affected by several factors, including surface roughness, connection preload, and the kind of substructures.

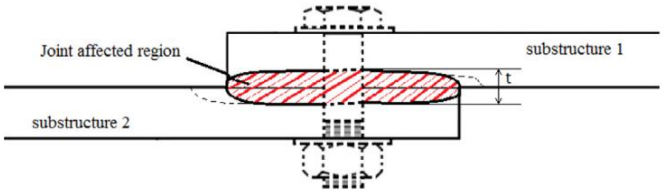

Fig. (3) The region where the screw connection is felt [7]

Three-dimensional connecting pieces with unidentified attributes are used to model the connection's impacted zone in Figure 3. The connecting layer's elastic characteristics, which are determined and modified in light of the experimental findings, serve as the model's parameters. The substructures are not layered; hence the structure's dimensions have not altered. Additionally, because the density of the components is considered to be equal to that of the substructure elements in the connection-affected region, the structure's overall mass is unaffected. Shokrollahi *et al*. have effectively applied this concept [15]. This model has been used by Shokrallahi and Adel to simulate the dynamic behavior of bolted joints in steel/steel and aluminum/aluminum constructions [16].

3. Case study

Figure 4(a) depicts the tested sample as two arrow-shaped blades fixed to a shared base, which is itself represented by a rigid disk [11, 17]. It has also been used in experiments that are similar to the one in which this laboratory sample was used, but in that experiment, the laboratory sample was suspended, allowing the experiment to be carried out in a free-free condition.

Figure 4(b) illustrates the wedge-shaped damper utilized in the test model, which has a triangular cross-section with a certain angle. The airfoil of the laboratory model is swapped out for a beam with a straight rectangular cross-section, in contrast to the airfoil of actual high-pressure turbine blades. The shape of the pseudo-blades is created to mimic the dynamic response of a genuine blade in order to make sure that these simplifications do not result in differing nonlinear dynamic behavior. The advantages of providing such a model in finite element simulation are discussed in Section 4, which describes the finite element model.

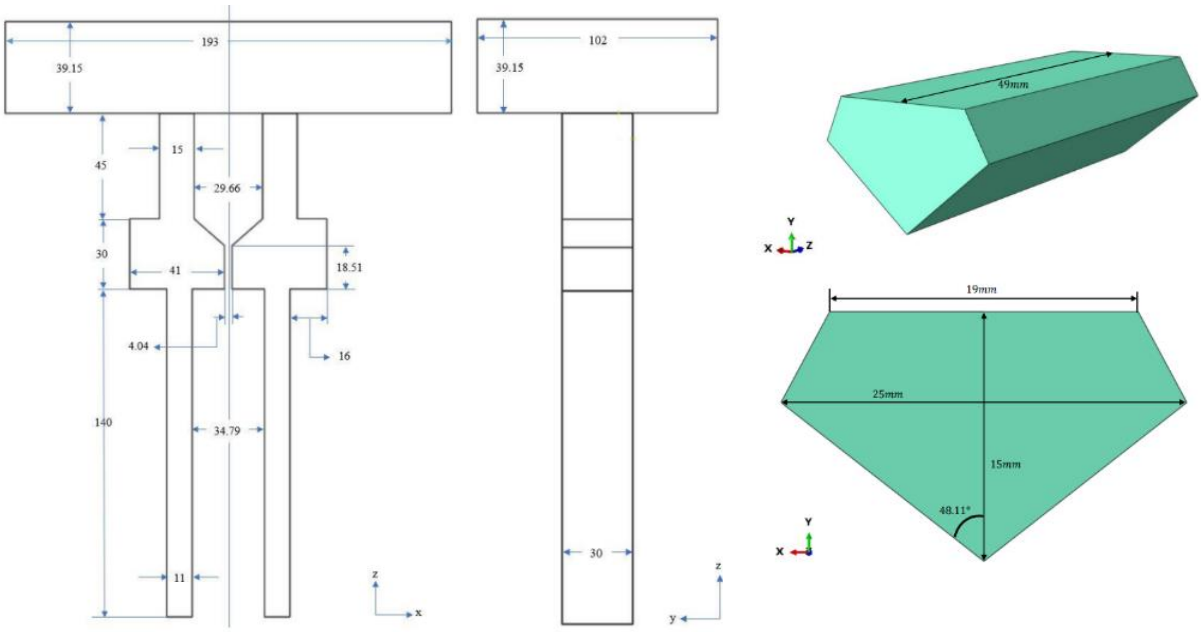

(a) (b)

Fig. (4) Schematic and dimensions of the structures (all of the measurements are in mm)

Figure 4(a) depicts the model's geometric features, which include a 15 cm deep base and 3 cm deep blades on each side. Two blades must be separated by 5.4 cm at the very least. The seats for the friction damper are spaced apart between the two blades. There is a 96° angle between the two blades. This open area represents 33 percent of the blade's length away from the base. Located between the seats is the damper.

Additionally, Figure 4(b) shows that a spring has been utilized to connect the wedge with the two-bladed platforms in order to replicate the centrifugal force on the wedge that is brought on by the circular movement. The laboratory model with the flexibility to vary its structure is made more practical and capable of producing diverse outcomes. Table 1 introduces the physical characteristics of the laboratory sample under investigation.

Table. (1) Physical characteristics of the lab sample

Segment	Value
E(Gpa)	210
ϑ	0.3
$\rho\left(\mathrm{kg.m^{-3}}\right)$	7800

4. Finite element model

The following assumptions are taken into account during the modeling process:

- The structure's mass and size are assumed to be constant.
- It is possible to simulate the dominant properties in the vibration behavior, such as reducing the stiffness in the connection area.
- The created model may be used for big structures
- The number of model parameters is kept to a minimum so that they can be determined with scant experimental data.

The model simulation was performed using the Abaqus finite element software. Steps included drawing different parts, assembling the parts and determining the material specifications by creating a combined type of elements. A total of 19870 elements including 19800 elements of C3D8R type and 70 elements of B31 were used. Also, determination of finer elements in the connection area according to Figure 5 and implementation of the model and presentation of its results have been discussed.

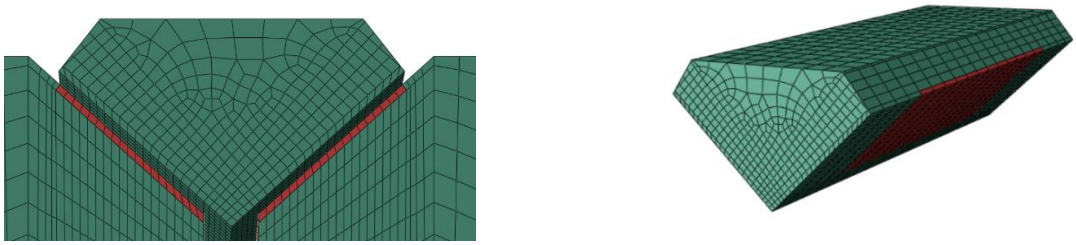

Fig. (5) Finite element software meshing of connecting area

Figure 6(a) depicts the completed model's construction. When compared to the integrated three-dimensional model, the airfoil of the laboratory sample is modeled using a beam with a straight rectangular cross-section (see Figure 6(b)). Additionally, with this modeling and taking the number of iterations required to update the final model into account, the execution time of the finite element software is decreased by roughly 87%.

(a) (b)

Fig. (6) Assembling the final airfoil model: (a) integrated 3D model, (b) beam model

5. Experimental analysis

The experimental setup, depicted in Figure 7, consists of two steel beams that are arranged to mimic the configuration of two turbine blades and the beams are fixed onto a base. To replicate the centrifugal force that occurs during the operation of the damper and is experienced by the blades, a spring force is applied to the experimental setup. The spring is initially deformed, and its stiffness results in the generation of a normal force.

Free-free boundary conditions are used for the assembled structure by suspending them as shown in Figure 7. Figure 7 depicts the stimulation of the tested structure by a TV52110-GMBH TIRA shaker and a steel stinger that is positioned close to the damper and at a distance of the one third of the blade from the base. To measure the excitation force, a B&K 8200 piezoelectric force transducer is placed between the structure and the stinger. A piezoelectric accelerometer with model number 120V-2778A-DJB is used to measure the response of the stimulated structure at the end of the blade. The structure is excited by a shaker at the junction between two blades with random signals excitation.

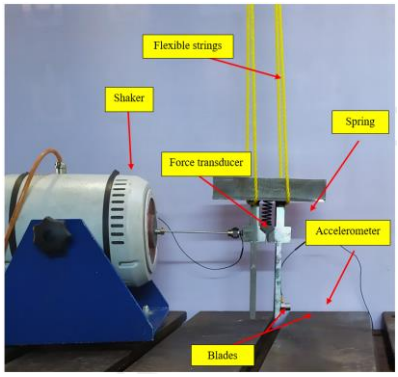

Fig. (7) Test set-up of the assembled structure

Figures 8 and 9, respectively, display the findings of the measured frequency and phase responses. Figuring out how to express the real and imaginary portions of the phase response in accordance with Figures 10-a and 10-b makes it easier to identify the system's natural frequencies so that a change in the imaginary part may be used to pinpoint the location of frequencies.

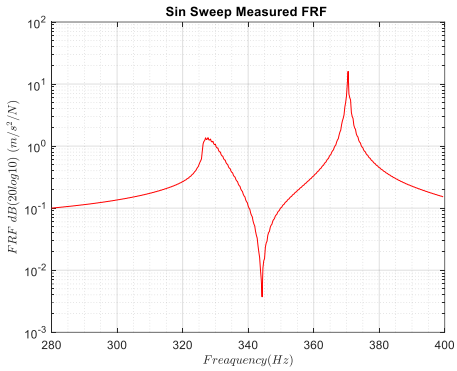

Fig. (8) Frequency response function from the experimental test (Inertance)

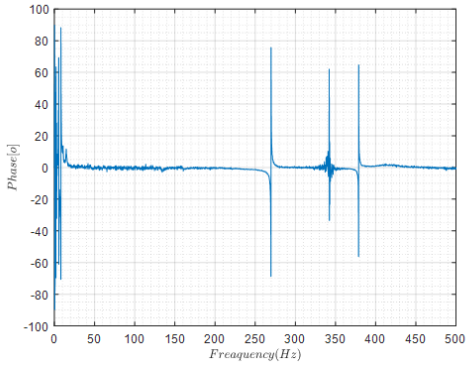

Fig. (9) Phase response from experimental test

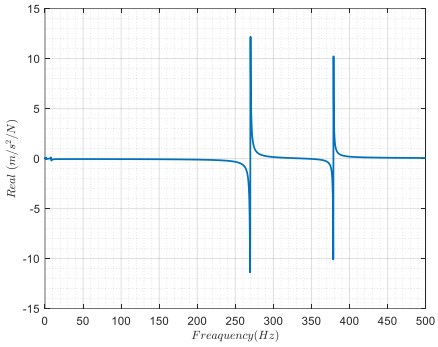

(a)

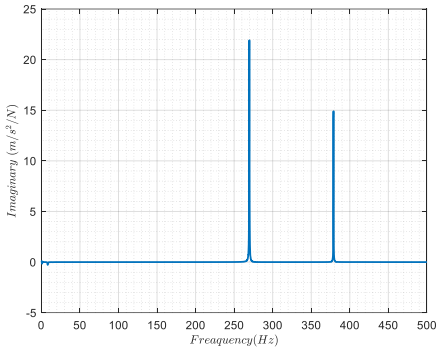

(b)

Fig. (10) Phase response: (a) real part, (b) imaginary part

The first and second natural frequencies of the modal test are shown in Table 2.

Table. (2) Two natural frequencies from experimental results

$\boldsymbol{\omega}_1^{(e)}(Hz)$	327
$\boldsymbol{\omega}_2^{(e)}(Hz)$	370.5

6. Model updating

6.1. Optimization algorithm

By reducing the disparity between experimental and numerical findings, parameters are identified. The approach used most frequently is to reduce the squared discrepancy between experimental and

numerical findings [18]. In optimization, a two-objective genetic algorithm with a population of 12 samples, a mutation rate of 0.2, a crossover rate of 0.9, and 200 iterations were executed. The difference of the squared error of the first and second natural frequencies of the structure from experimental and numerical data is one of the cost functions that were chosen.

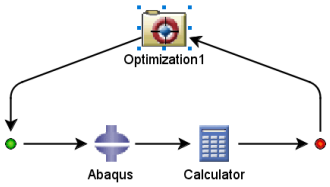

Fig. (11) The optimization cycle formed in Isight software

The software optimization module for Isight determines the connection settings. Using the system's first two natural elastic frequencies, which are defined in relation 1, the relationship between the Abaqus software and the two objective functions, which are defined as the cost function in the software calculator, are shown in Figure 11 after the desired parameters have been defined. The multi-objective genetic algorithm will be used in this stage to construct an optimization approach in the Isight software's optimization solver.

$$\boldsymbol{F} = \left| \frac{\boldsymbol{\omega}_i^{(n)}}{\boldsymbol{\omega}_i^{(e)}} - \mathbf{1} \right| \qquad \boldsymbol{i} = \mathbf{1}, \mathbf{2} \qquad \rightarrow \qquad \mathbf{min}\ (\boldsymbol{F}) \tag{1}$$

where $\omega_i^{(n)}$ and $\omega_i^{(e)}$ represent the natural frequency deriving from finite element modeling and experiments.

6.2. Different levels of connection area

The damper surfaces of the system are not always linked to the sub-platform and not all connection areas are included in this section. It is dependent on the physics of the issue and the kind of connection, particularly in the form of the second elastic mode. To choose the best shape of the surface under the connection, the parameters of the surface under the influence of the connection are identified, and the results of the objective functions of the minimum state of each model are compared, as shown in Table 3. As a result, three types of the joint affected region, rectangular and ellipsoidal and two-piece shape models are considered, with each of them being considered in five different sizes (next section).

Table. (3) Three types of joint affected region, rectangular and ellipsoidal and two-piece shape in five different sizes

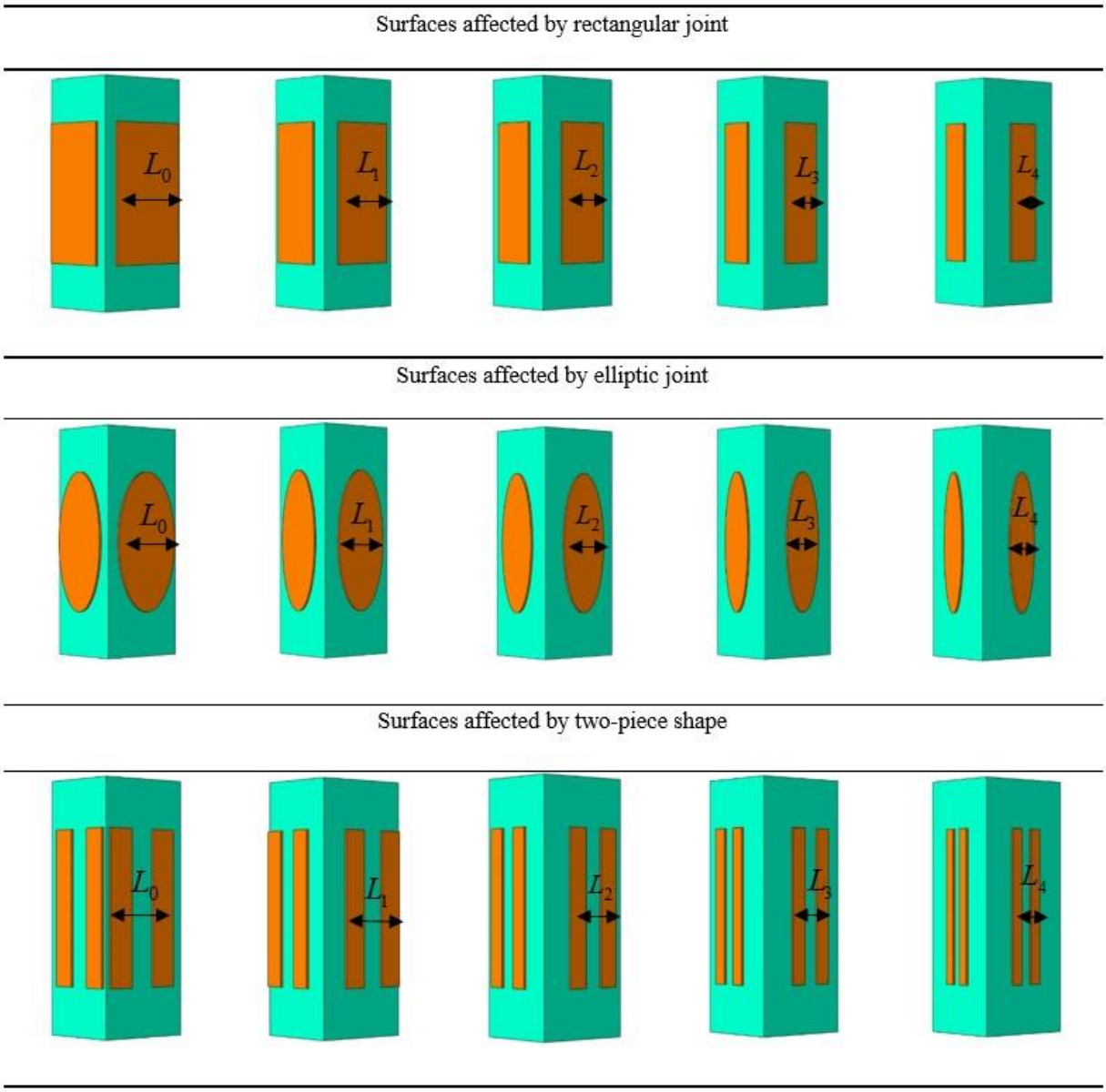

7. Simulation results

Following cost function optimization and minimization, it is possible to compare the optimized cost function results. In other words, the error of the 10 models introduced in the preceding section, which in some way illustrates how far the natural frequencies of the model are from the test results, can be measured by summing the minimum error of each model. The connection effect offers the option to select the optimal surface form.

Figures 12 to 14 respectively illustrate the outcomes of the minimum error comparison of the oval, rectangular and two-piece models. Evidently, as the surface under the connection's influence

grows, the error also grows. This demonstrates that similar to the physics in the problem, not all of the connection's initial surface will have the same frictional effect, and the central contact surface will predominate.

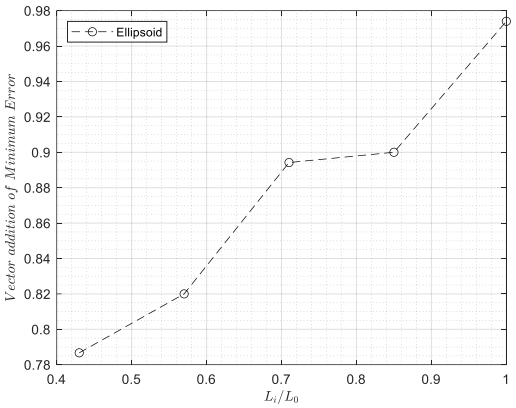

Fig. (12) The Optimized Ellipsoid surface under the influence of connection

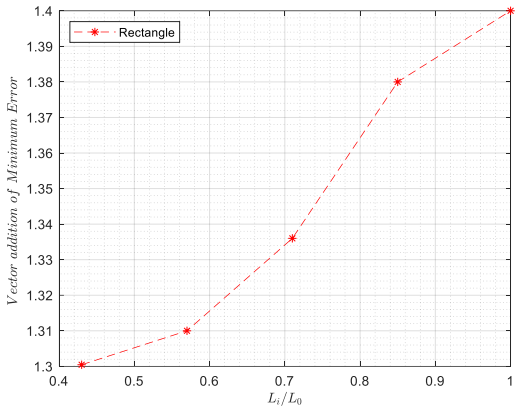

Fig. (13) The Optimized Rectangle surface under the influence of connection

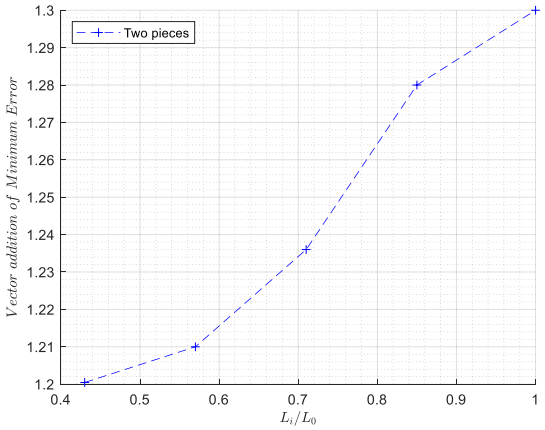

Fig. (14) The Optimized Two pieces surface under the influence of connection

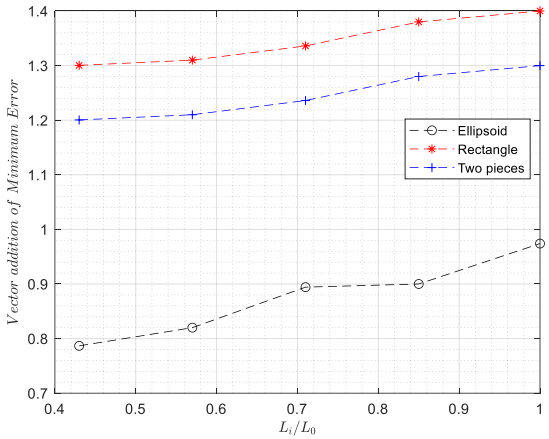

Fig. (15) Comparison of surfaces under the effect of optimized rectangular and elliptic and two pieces connection

It can be shown by contrasting the results of the rectangular, elliptical and two-piece joint surfaces in Figure 15 that the elliptical results consistently and at each L_i/L_0 are better able to forecast the test results and, as a consequence, have less error than the results of rectangular surfaces.

8. Conclusion

Comparison of the simulation results of the finite element method with the results of the experimental test shows that the surface under the influence of the oval connection behaves better than the rectangular shape and two-piece. In all three cases, a better simulation behavior will be offered as the surface under the effect decreases and gets closer to the center of the effect.

This paper presented an experimental investigation of the joint affected region of under-platform dampers in mechanical engineering. The aim was to identify the physical and geometrical properties of the surfaces affected by the connection in order to minimize errors caused by the selection of the contact surface type. The study focused on two blades and a damper under a wedge-shaped platform, which is free-free, and the behavior of the surfaces affected by the connection was optimized based on results obtained from experimental testing and finite element modeling. The investigation considered three types of affected surfaces - rectangular and oval and two pieces - in five different dimensions to determine the optimal model and dimensions of the affected surface. By updating the connection properties, this study aimed to improve the performance of under-platform dampers in reducing vibrations and enhancing the stability of mechanical structures.

The results indicate that, in terms of the ability to bring finite element simulation results closer to experimental test results, the elliptical connection's affected area performs better than the rectangular and two-piece connections. Furthermore, reducing and centering the affected surface in all three cases leads to improved simulation behavior. Therefore, optimizing the affected surface geometry and positioning it at the center of the effect can enhance the performance of under-platform dampers and reduce vibrations in mechanical structures.

References

[1] E. Seinturier, Forced response computation for bladed disks industrial practices and advanced methods, Lecture Series-Von Karman Institute For Fluid Dynamics, 2 (2007) 5.

[2] L.M. Amoo, On the design and structural analysis of jet engine fan blade structures, Progress in Aerospace Sciences, 60 (2013) 1-11.

[3] Z. Qu, D. Hu, Z. Chen, Contact nonlinear analysis for the under-platform dampers of blade based on a frictional energy dissipation model, in: Structures, Elsevier, 2021, pp. 146-155.

[4] D. Ewins, Control of vibration and resonance in aero engines and rotating machinery–An overview, International Journal of Pressure Vessels and Piping, 87 (2010) 504-510.

[5] J. Griffin, Friction damping of resonant stresses in gas turbine engine airfoils, Journal of Engineering for Power, 102 (1980) 329-333.

[6] T. Cameron, J. Griffin, R. Kielb, T. Hoosac, An integrated approach for friction damper design, (1990).

[7] E. Petrov, A method for use of cyclic symmetry properties in analysis of nonlinear multiharmonic vibrations of bladed disks, J. Turbomach., 126 (2004) 175-183.

[8] K. Sanliturk, M. Imregun, D. Ewins, Harmonic balance vibration analysis of turbine blades with friction dampers, (1997).

[9] B. Yang, M. Chu, C. Menq, Stick–slip–separation analysis and non-linear stiffness and damping characterization of friction contacts having variable normal load, Journal of Sound and vibration, 210 (1998) 461-481.

[10] E. Cigeroglu, W. Lu, C.-H. Menq, One-dimensional dynamic microslip friction model, Journal of Sound and Vibration, 292 (2006) 881-898.

[11] K.Y. Sanliturk, D.J. Ewins, A.B. Stanbridge, Underplatform dampers for turbine blades: theoretical modeling, analysis, and comparison with experimental data, J. Eng. Gas Turbines Power, 123 (2001) 919-929.

[12] E. Ciğeroğlu, H.N. Özgüven, Nonlinear vibration analysis of bladed disks with dry friction dampers, Journal of Sound and Vibration, 295 (2006) 1028-1043.

[13] M. Allarà, A model for the characterization of friction contacts in turbine blades, Journal of Sound and Vibration, 320 (2009) 527-544.

[14] J. Cao, J.L. Grenestedt, Design and testing of joints for composite sandwich/steel hybrid ship hulls, Composites Part A: Applied science and manufacturing, 35 (2004) 1091-1105.

[15] A. VanderKlok, A. Dutta, S.A. Tekalur, Metal to composite bolted joint behavior evaluated at impact rates of loading, Composite Structures, 106 (2013) 446-452.

[16] S. Shokrollahi, F. Adel, Finite element model updating of bolted lap joints implementing identification of joint affected region parameters, Journal of Theoretical and Applied Vibration and Acoustics, 2 (2016) 65-78.

[17] C.M. Firrone, Measurement of the kinematics of two underplatform dampers with different geometry and comparison with numerical simulation, Journal of Sound and Vibration, 323 (2009) 313-333.

[18] M. Bazrafshan, H. Ahmadian, H. Jalali, Modeling the interaction between contact mechanisms in normal and tangential directions, International Journal of Non-Linear Mechanics, 58 (2014) 111-119.